MODELLING MULTISTATIC OF TARGET DETECTION

ZYGMUNT KLUSEK*, ANDRZEJ ELMINOWICZ**,
JAROSŁAW TĘGOWSKI*, JOANNA SZCZUCKA*, AGATA DRAGAN*

*Institute of Oceanology, PAS, ul. Powstancow Warszawy 55, 81-712 Sopot, POLAND
** R&D Marine Technology Centre, ul. Dickmana 62, 81-109 Gdynia, POLAND
klusek@iopan.gda.pl

The paper presents a numerical approach to modelling the detection of underwater targets with a bi- or multistatic active sonar systems in the shallow water areas using different waveform signals. The results of the numerical modelling of surface, bubble clouds and bottom reverberation for CW and using up and down time-varying instantaneous frequency of chirp signals are presented. Some suggestions are made on the basis of the development and practicality for the shallow sea modeling techniques and approaches to existing sonar models. The paper reports the literature of the model components required for active sonar modelling for different propagation conditions. Some examples of scattering of CW and chirp source signals at bubble clouds and corrugated surfaces, and coherence are given. Active propagation and the system performance are surveyed and modelled adaptable to the specific environmental condition of the shallow sea area of the Gdansk Gulf.

INTRODUCTION

Introduction of an underwater hydroacoustic security system to a specific area, in order to predict a reliable detection of the underwater targets at safe distances, requires carrying out the investigations of acoustic propagation conditions and/or performing a numerical modelling. As a part of the project employing a system composed of bottom mounted and ship-borne active sonars at its initial phase, it is supposed to provide a numerical simulator of target detection. Such modeling should be also undertaken as part of a preliminary site selection process.

The model should maintain, specific for the area, volume, sea bottom and surface reverberation, propagation conditions and their statistics, climatic condition models, spatial and temporal coherence of sound speed field and finally target properties

To support these requirements, also some measurements of the basic environmental parameters of sound propagation are to be planned to generate the input data into the model.

Due to the planned frequency range of signals, between 50 and 90 kHz, the most suitable model used to predict propagation is the acoustic geometrical approximation.

Because of the complexity of the acoustic propagation and 3D scattering at boundaries in shallow water at this phase of model development, the individual components of models are considered and individual scenarios repeatedly played to receive the qualitative results.

Taking into consideration the accessible models of scattering at the sea bottom and the sea surface, it should be keep in mind that the published models are usually performed for CW waves – where the information about a coherent component of the scattered signals does not play a vital role ([5, 6,7,17]).

The apparent shortcomings of the existing models (as example [9]), from our point of view, in particular, are lack of reliable biscattering models in the investigated here frequency range ([1,9,11,15,16]), both for CW and chirp sounding signals.

In the system, we take the signal compression approach to analyze the probability of the detection of a target and estimate the level of reverberation. In the pulse compression processing, we compute the cross-correlation between the signal received from all reflections and scattering and the reference signal from output of the transmitter.

Due to relatively high frequency range of the soundings signals, the bottom penetration phenomena are neglected.

The suitability and fidelity of the active sonars modelling in the frequency band in question and for wideband signal character, will be evaluated in the future on the basis of planned experiments in the area of interest.

This paper presents the submodels applicable to active modelling of the chirp type signals in the Baltic Sea in the high frequency range. Procedures include propagation modelling in the specific environment, volume reverberation modelling, scattering from sea surface (jointly with bubble clouds), bottom and volume inhomogeneities. The equally essential problem is our ability to appropriate modelling targets.

Above this, diffuse scatterers as fish and bubbles forming the different form of swarms, plumes and clouds are included into the model.

The very important question the model is recognition of relatively poor identified problem in hydroacoustics – which rate of scattered wave energy constitutes the coherent component which determines our ability to detect targets.

1. SIGNAL AND PROPAGATION MODELLING

The assuming workhorse signals are the linear frequency modulated signals

$$p(t) = a_0(t)\exp\left(-i\left(\omega_0 t \pm (\dot{\omega}/2)t^2\right)\right), \qquad (1)$$

where ω_0 is the initial frequency at t=0, $\dot{\omega}$ is the frequency-sweep rate of the signal and $a_0(t)$ the amplitude. We assume that the amplitude is equal beyond the time t=T – signal duration, the ± sign means that the instantaneous frequency of the chirp signal could be going up or down. In practice, the duration T is of the order of tens of miliseconds, which results in the frequency-sweep rate in the range of 25-50 kHz/s.

A universal equation for the bistatic boundary scattering of a signal in the ray approximation can be written in the form:

$$p(t) = \iint_{A(\vec{r})} \sum_i \sum_j p_{0,i,j}\left(t - t_{i,j}\right) P_i \, P_j \, \sigma_S\left(\theta_i, \theta_j, \varphi\right) \sigma_B\left(\theta_i, \theta_j, \varphi\right) dA_S \, dA_B \qquad (2)$$

where indexes i and j refer to all rays departing the transmitter and registered at the receiver, *dA*s are the elemental scattering areas at the sea surface and the sea floor for the rays with indexes i and j. The *P* means the propagation term of individual rays. The scattering properties of the rough boundaries are described by 3D local scattering functions S_S and S_B.

An effect of changing the spectrum of the signal travelling through the waveguide along one path could be written as:

$$p(t) = \int_0^\infty \prod_i R_b(\omega) R_s(\omega, t) V_s(\omega, t) \exp(i\omega t) d\omega \qquad (3)$$

where $V_s(\omega,t)$ is the spectrum of the emitted signal, and $R_b(\omega;r)$ and R_s $(\omega; t)$ are the reflection coefficients at the sea surface and sea bottom. The $\prod$ reflects the fact of multiple reflections at the boundaries. In the formula, the dependence of scattering on the incident and scattering angles are not marked explicitly. Pulses reflected (scattered) from the bottom and the sea surface, together with the rays scattered at the target are coherently summed at the receiver

Due to the bandwidth of the chirp, the compression at the receiver unit acts as a bandpass filter suppressing other signals, as well the Doppler return from moving inhomogeneities in the water masses. At this stage of the model development, because of poor knowledge of the input random component in the sound speed along a ray, we low-pass filter vertical profiles of the sound speed.

The simulations presented below demonstrate some examples of properties of scattered LFM signals at rough boundaries and bubble clouds.

2. BUBBLES REVERBERATION

The signal volume scattering is predominantly caused by bubbles or zooplankton and fishes. In theory, the volume reverberation at randomly distributed scatterers should have a negligible coherent component and therefore can be ignored ((12,13]).

The scenario presented below simulates a response of a bubble cloud of the known concentration, the size spectrum and the given size distribution with the depth to the chirp sequences. The frequencies of the chirp signal are only partly tuned to the bubbles resonant frequencies. Numerical experiments were designed to compare the sequence of echoes from CW and LMF signals from evolving a bubble plume, to identify potential benefits from chirp signals.

A classical Rayleigh-Plesset model was used to estimate the acoustic response of a single microbubble. Compared with typical CW sounding pulses, chirps are usually long in duration, so are able to carry more energy without increasing the amplitude, but on the other side maintaining a wide bandwidth.

Estimations performed on the basis of data concerning bubble concentrations in the Baltic Sea provide values of sound attenuation inside of fresh plumes of order of tens dB/m. So, only a thin shell of bubbles on the cloud surface participates in the sound scattering. We assume that the size spectrum of bubbles obeys the power law distribution (Fig.1).

The geometry of a presented example is illustrated in Fig.2, and some important parameters of the echo as the spectrum and coherent component time dependence are given in Figs. 3 and 4. The parameters of the source are: signals amplitude at r=1 m P_0=10000 Pa, distance to the bubble plume L=30 m. The plume is simulated as a set of point scatterers positioned inside of an

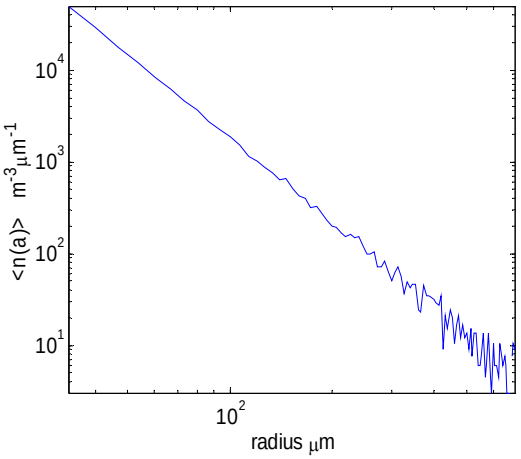

Fig.1 Example of bubbles size distribution inside a bubble cloud, $n(a) \approx a^{-3}$

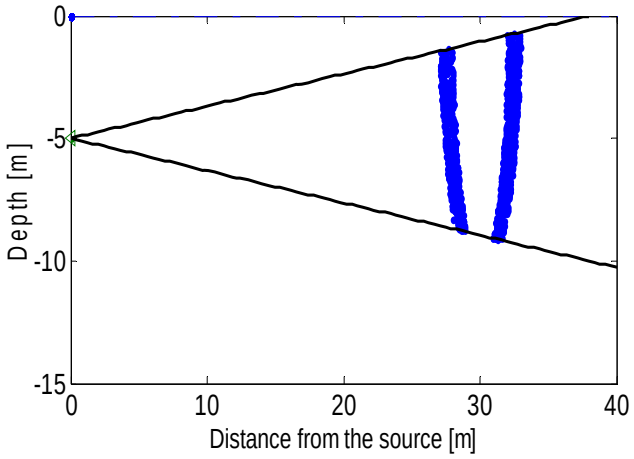

Fig.2 Geometry of backscattering at a bubble cloud

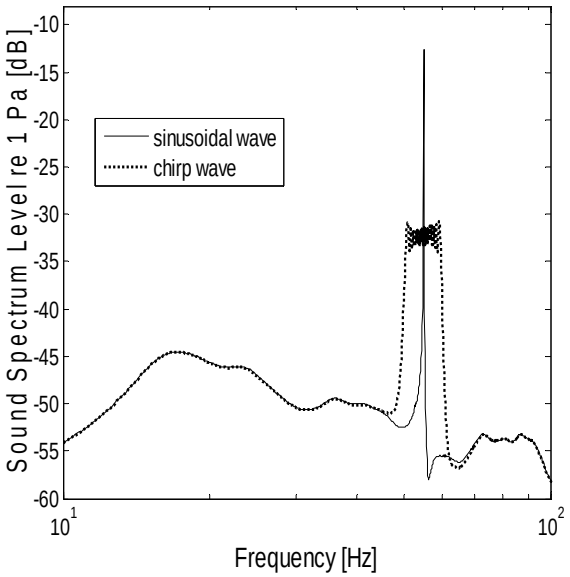

Fig.3 Spectra of backscattered CW and LFM signals from a bubble cloud, with power law size spectrum, as above $n(a) \approx a^{-3}$

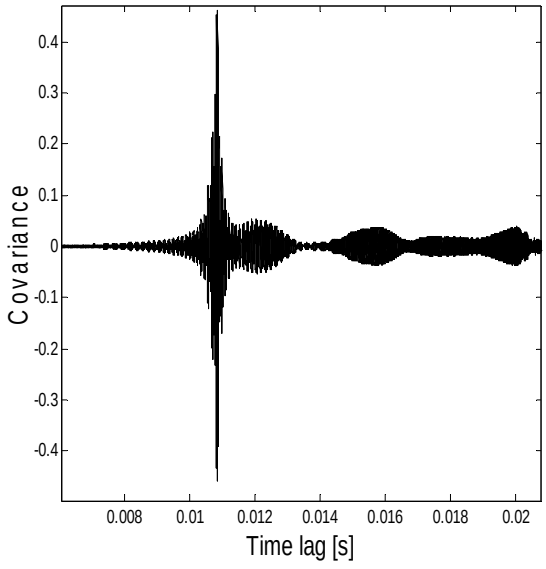

Fig.4 The cross-correlation of a backscattered at a bubble cloud signal with its replica at the output of the transmitter

ellipsoidal semicylinder with axes equal – the horizontal axis 3m and the vertical one 10m. The transducer's acoustic axis is perpendicular to the axis of the cylinder. The value of the concentration of bubbles is chosen so that the mean sound attenuation in the frequency band 50-60 kHz is equal 30 [dB/m]. The profile of concentration with the depth is exponentially decaying.

The influence of bubble clouds on sound propagation consists mainly of scattering and attenuation. For low and moderate wind speed for frequencies of interest i.e. 50 - 60 kHz, the value of the sound-speed perturbation are very small, comparing to the sound speed in the pure sea water (the ratio of $\Delta C/C_0$ is of the order of 10^{-2}).

On the basis of numerical simulations we could state that for dense bubbles clouds early backscattering can be highly coherent due to backscattering at a relatively thin bubble layer at the cloud boundary. The coherence is quickly diminishing when later volume reverberation is increasingly uncorrelated.

3. SURFACE AND SEA BOTTOM SCATTERING MODELS

In the programme different surface models were tested. The surface models include that the scattering is composed of two types of interactions: reflections from planes and facets of large-scale roughness and resonant interactions from small-scale roughness. When we assume that the surface roughness spectrum is continuous and contains irregularities of all sizes some threshold value should be set up to distinguish between two types of scattering.

The statistical properties of the facets distribution could by described by two dimensional spectra of wave numbers or using fractal dimension. The last one representation is suggested as more realistic, due to the fact, those sea-floor roughness exhibit features at many different scales of length they could be described as fractals. ([2,3])

At angles near normal and for forward scatter, the boundary could be composed of the 2D the large-scale roughness features. As parameter we put either the RMS slope of the surface or the RMS height and correlation length on which are placed small facets. Facets provide planes which specularly scatter sound. Though this kind of model is well suited to bistatic scattering prediction, we simplify the problem assuming only specular (geometrical) reflection. To receive the significant number of rays crossed the area of the receiver, the facets number should be of the order of 10^6. Similar problems arise when the rough surface is described using fractals.

Scattered intensity from any facet is described by the scattering cross-section $\sigma_b(\theta_s, \phi_s, \theta_i)$ which belongs to the acoustic parameters of the ocean bottom.

For surfaces with Gaussian statistics and narrowband signals, the application of this type of model to forward scatter has been proven successfully modelling high angle backscatter on both the ocean surface and the ocean bottom [4].

Scattering coefficient depends on the θ_i which is the angle of incidence of a plane wave (elemental beam) at the bottom and θ_s, ϕ_s are the scattering angles for an actual beam of observation angle, and the bottom character based on the sediments granulometric characteristics.

Bistatic scattering coefficient is defined as follows:

$$S_b(\theta_s, \phi_s, \theta_i) = \sqrt{\sigma_{br}(\theta_s, \phi_s, \theta_i)}, \qquad (4)$$

where: σ_{br} – the rough surface scattering cross section, θ_s, ϕ_s – the azimuth and vertical scattering angles and θ_i - incidence angle.

We developed a series of algorithms in terms of the broken mirror approximation to express the high angle reflectivity from facet-like planes (following the physics of the Kirchhoff-Helmholz equation).

In the bistatic applications the facet's set requires two coefficients - the facet strength (the sediments reflection loss at a normal incidence) and surface statistics as - the facet size or RMS slope which could be assumed as a Gaussian random surface or have fractal properties.

The reflection losses dependent on sediments grain size are taken from the APL/UW High frequency models Handbook [8] . However, exceptionally extensive concerning sediments character and the frequency regime, the validity of the scattering strength in the APL/UW High frequency models was tested for CW signals (The Mourad/Jackson model).

Backscatter and biscatter categories in the case of summing of coherent scattering cannot be modeled using only as the scattering parameter the differential scattering cross-section of the each facet. The 3D directivity function was introduced for each facet and calculated for the each element for given angle of incidence and the angle of scattering. However improving the results statistic comparing to the simple geometrical reflection from a broken mirror, the computational effort is very high.

Another implemented model of the rough scattering surface is the point scatteres model. The surface is defined as the equidistant mesh of points with Gaussian distribution of deflection from the mean surface. The set of the z coordinates of the points is generated using 2D low pass filters for a set of random values. The roughness spectra are very similar in both perpendicular directions. The source directivity functions was modeled here as an ideal conelike beam.

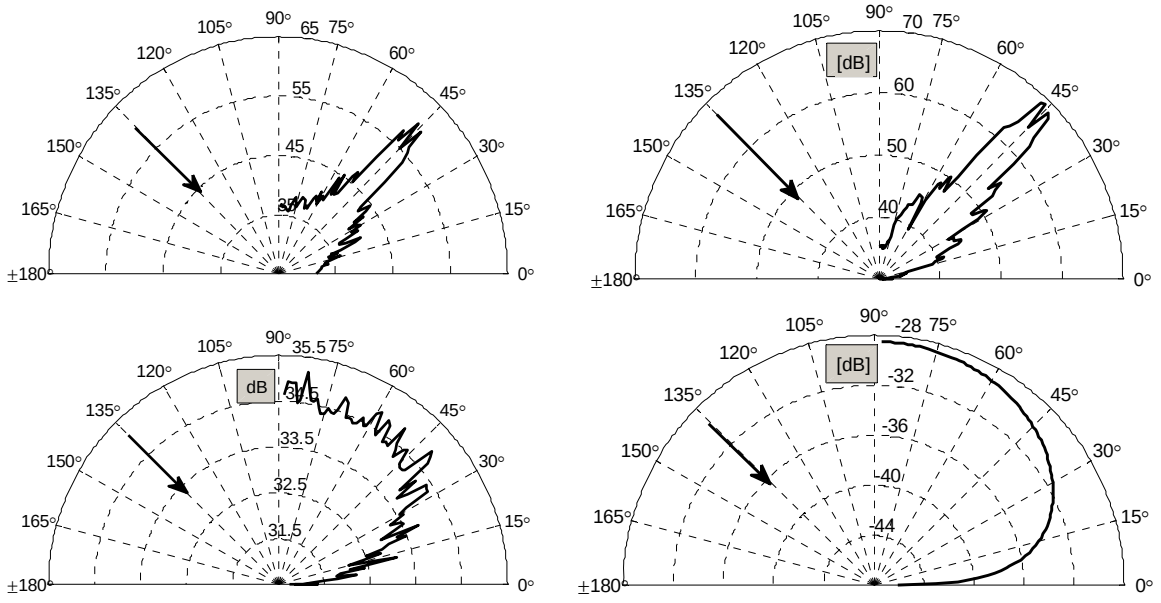

Fig.5 The test data concerning the forward scattering of different signals at the rough surface using the point scattering model. The signals and surface roughness are a) CW signal, $\sigma=\lambda/20$; b) LFM signal, f1=50, f2=60 kHz, $\sigma=\langle\lambda\rangle/20$; c) CW signal, $\sigma=5\lambda$; d) Lambert Rule for strongly rough bottom

4. SOUND SPEED FIELD FLUCTUATION STATISTICS

Fluctuations in acoustic pressure amplitudes (variations about some mean level) are caused by many processes at sea such as randomness of sound speed inside the propagation channel, surface motion, internal waves, etc. However, our knowledge about the proper statistics of physical field which generate the reverberation and noise portions of scattered and far range propagated signals is unsatisfactory.

In case of broadband postprocessing the Doppler spectral spread from the moving sea surface and surface bubble motion could be observed [14]. However, a roughly estimation of the effect gives values Δf of some tens of Hz for the highest frequencies. So, this effect would only be important for shorter signals and the upper range of frequencies.

5. TARGET MODELS

In the used frequency regime when wavelengths are smaller than 5 cm, the significant role in the coherence of the scattered signal plays the shape of any realistic target. Above the scattering at the diver's body or equipment we should take into consideration significant scattering centers at gas plume.

6. SUMMARY

This paper goes over several components of the active multistatic systems modelling and waveform time series propagation. Some recommendations concerning the placement of the transmitters and receivers could be made on the repeatedly played scenarios of the sound propagation under different statistics of reverberation, propagation and weather conditions, source models, fluctuation statistics, spatial and temporal coherence, spreading functions and target strength.

At the present stage of development of the simulator the environmental scene was modeled as though the model was a collection of homogeneous regions plus simply targets.

We expect that the preliminary results represent a good starting point for simulation of a target detection using the chirp signals in realistic environment.

ACKNOWLEDGMENT

This work is financed by grants O R00 001804 dedicated for research and development by the Ministry of Science and Higher Education.

REFERENCES

1. M. Badiey, M. Yongke, J. Simmen and S. Forsythe, Signal variability in shallow-water sound channels" IEEE Journal of Oceanic Engineering, Vol 25, No 4, 492- 500, 2000.
2. F. Berizzi, E. Dalle-Mese, Scattering from a 2D sea fractal surface: fractal analysis of the scattered signal, Antennas and Propagation, IEEE Transactions on Vol 50, 7, 912 – 925, 2002.
3. B. Birkhäuser, Fractal reconstruction of sea-floor topography, Vol. 131, 1-2, 197-210, 1989.

4. B. Cole, J. Davis, W. Leen, W. Powers, J. Hanrahan, Coherent bottom reverberation: Modeling and comparisons with at-sea measurements, J. Acoust. Soc. Am. Vol. 116, No. 4, 1985-1994, 2004.
5. J. W. Caruthers, J. C. Novarini, Modelling Bistatic Bottom Scattering Strength Including a Forward Scatter Lobe, IEEE J.O.E., 18(2): 100-107, 1993.
6. P. Dahl, High frequency forward scattering from the sea surface: the Characteristic scales of time and angle spreading, IEEE Journal of Oceanic Engineering, Vol. 26 No 1 141-151, 2001.
7. D. E. Dale, D. V. Crowe, Bistatic Reverberation Calculations Using a Three-dimensional Scattering Function, J. Acoust. Soc. Am. 89:2207-2214, 1991.
8. C. Eggen, K. Williams, APL-UW High-Frequency Ocean Environmental Acoustic Models Handbook, Applied Physics Laboratory, University of Washington, 1994.
9. K. Gilbert, A Stochastic Model for Scattering from the Near Surface Oceanic Bubble Layer, J. Acoust. Soc. Am. 94(6): 3325-3334, 1993.
10. P. C. Hines, D. V. Crowe, D. D. Ellis, Extracting in-plane bistatic scattering information form a monostatic experiment, J. Acoust. Soc. Am. 104(2, part 1): 758-778, 1998.
11. K. LePage, Bottom reverberation in shallow water: Coherent properties as a function of bandwidth, waveguide characteristics, and scatterer distributions, J. Acoust. Soc. Am. 106(6): 3240- 3254, 1999.
12. S. T. McDaniel, Sea surface reverberation: A review, J. Acoust. Soc. Am. 94(4): 1905-1922, 1993.
13. S. T. McDaniel, D. F. McCammon, Composite Roughness Theory Applied to Scattering from Fetch Limited Seas, J. Acoust. Soc. Am., 82(5): 1712-1719, 1987.
14. D. F. McCammon, S. T. McDaniel, Spectral spreading from surface bubble motion, IEEE Journal of Oceanic Engineering, Vol. 15, No. 2, 95-100, 1990.
15. J. R. Preston, W. A. Kinney, Monostatic and bistatic reverberation results using linear frequency-modulated pulses, J. Acoust Soc. Am. 93(5): 2549-2565, 1993.
16. H. Schmidt, J. Lee, Physics of 3-D scattering from rippled seabeds and buried targets in shallow water, J. Acoust. Soc. Am. 105, 1605-1617, 1999.
17. K. L. Williams, D. R. Jackson, Bistatic bottom scattering: Model, experiments and model/data comparison, J. Acoust. Soc. Am. 103(1): 169-181, 1998.